Original Article

JCBFM

Journal of Cerebral Blood Flow & Metabolism
2017, Vol. 37(12) 3774–3788

DOI: 10.1177/0271678X17712178
journals.sagepub.com/home/jcbfm
SAGE

Protein kinase C epsilon delays latency until anoxic depolarization through arc expression and GluR2 internalization

Charles H Cohan[1,2,3,4], Holly M Stradecki-Cohan[1,3,4], Kahlilia C Morris-Blanco[1,3,4], Nathalie Khoury[1,3,4], Kevin B Koronowski[1,3,4], Mehdi Youbi[1,3], Clinton B Wright[2,3,4] and Miguel A Perez-Pinzon[1,2,3,4]

Abstract

Global cerebral ischemia is a debilitating injury that damages the CA1 region of the hippocampus, an area important for learning and memory. Protein kinase C epsilon (PKCε) activation is a critical component of many neuroprotective treatments. The ability of PKCε activation to regulate AMPA receptors (AMPARs) remains unexplored despite the role of AMPARs in excitotoxicity after brain ischemia. We determined that PKCε activation increased expression of a protein linked to learning and memory, activity-regulated cytoskeleton-associated protein (arc). Also, arc is necessary for neuroprotection and confers protection through decreasing AMPAR currents via GluR2 internalization. In vivo, activation of PKCε increased arc expression through a BDNF/TrkB pathway, and decreased GluR2 mRNA levels. In hippocampal cultured slices, PKCε activation decreased AMPAR current amplitudes in an arc- and GluR2-dependent manner. Additionally, PKCε activation triggered an arc- and GluR2 internalization-dependent delay in latency until anoxic depolarization. Inhibiting arc also blocked PKCε-mediated neuroprotection against lethal oxygen and glucose deprivation. These data characterize a novel PKCε-dependent mechanism that for the first time defines a role for arc and AMPAR internalization in conferring neuroprotection.

Keywords

Brain ischemia, glutamate, hippocampus, ischemic preconditioning and induced tolerance, synapses, dendrites

Received 7 January 2017; Revised 29 March 2017; Accepted 26 April 2017

Introduction

Out-of-hospital cardiac arrests (CAs) affect approximately 400,000 people every year in the United States and have a survival rate of only 8%.[1,2] Survivors often suffer from brain damage and irreversible learning and memory deficits[3] as a consequence of the global cerebral ischemia-induced neuronal damage.[4] The lack of oxygen and glucose during cerebral ischemia results in a bioenergetics failure leading to a phenomenon known as anoxic depolarization (AD), a sustained and potentially irreversible depolarization of neurons.[5–7] Vulnerable regions of the brain, such as the CA1 region of the hippocampus, are often affected following ischemia[8,9] and cell death can occur.[10–12]

An effective neuroprotective strategy against cerebral ischemia is ischemic preconditioning (IPC).[13,14] IPC is the treatment of the brain with sub-lethal ischemia followed by a period of recovery prior to a lethal ischemic insult; the sublethal ischemia primes the brain resulting in neuroprotection. Previous research in our

[1]Cerebral Vascular Disease Research Laboratories, University of Miami Leonard M. Miller School of Medicine, Miami, FL, USA
[2]Evelyn F. McKnight Brain Institute, University of Miami Leonard M. Miller School of Medicine, Miami, FL, USA
[3]Department of Neurology, University of Miami Leonard M. Miller School of Medicine, Miami, FL, USA
[4]Neuroscience Program, University of Miami Leonard M. Miller School of Medicine, Miami, FL, USA

Corresponding author:
Miguel A Perez-Pinzon, Department of Neurology, D4-5, University of Miami Leonard M. Miller School of Medicine, P.O. Box 016960, Miami, FL 33101, USA.
Email: perezpinzon@med.miami.edu

laboratory determined that activation of the epsilon isoform of protein kinase C (PKCε) is necessary for the neuroprotective effect of IPC.[14,15] Also, the application of a specific activator of PKCε, ψε-Receptor of Activated C Kinase (ψεRACK), can be used as a neuroprotective, pharmacological mimetic of IPC, conferring neuroprotection 48 h after treatment.[14,15]

Previously, we showed that activation of PKCε with ψεRACK can also modulate the synapse by increasing the amplitude of miniature inhibitory postsynaptic currents (mIPSCs).[16] Other groups have shown a less specific PKCε activator, bryostatin (also promotes PKCα activation), increases spontaneous IPSCs in CA1 hippocampal neurons,[17] enhances synaptogenesis following stroke in neonatal rats,[18] and promotes survival in aged rats following stroke.[19] However, the specific activation of PKCε and its ability to confer neuroprotection through modulation of excitatory synapses has not previously been investigated.

In a recent study, we found that two days following an application of ψεRACK, BDNF protein expression increased, and this increase was linked to decreases in CA1 neuronal action potential firing rates and delayed the onset of AD during oxygen-glucose deprivation (OGD).[20] In the same study, nonspecific inhibition of Trk receptor signaling abolished IPC and ψεRACK induced neuroprotection. BDNF protects neurons against hypoxia through a mitogen activated protein kinase (ERK)/mitogen-activated protein kinase kinase (MEK)-dependent pathway.[21] This signaling pathway (i.e. BDNF/MEK/ERK) was also implicated in the increased expression of activity-regulated cytoskeleton-associated protein (arc).[22–26] Arc decreases AMPA receptor (AMPAR) number and current at excitatory synapses[27] and protects against the effects of an apoptosis inducing protein, Amida, in COS-7 cells.[28] The role of arc in preconditioning-induced neuroprotection has not previously been investigated. Therefore, we sought to test the hypothesis that PKCε-activation enhances BDNF expression and its known downstream signaling partner arc, thereby conferring neuroprotection against a lethal ischemic injury through an AMPAR-dependent mechanism.

Materials and methods

Animal care

All animal procedures were carried out in agreement with the Guide for the Care and Use of Laboratory Animals and approved by the Animal Care and Use Committee of the University of Miami. Animals were supervised and housed in facilities of the division of veterinary resources with free access to food and water. They were transported to the laboratory only for administration of anesthesia, experimental procedures, and to be sacrificed.

In vivo injections

Twenty-five-day-old male Sprague Dawley rats (Charles River Laboratories, Wilmington, MA, USA) were injected intraperitoneally (i.p.) with the PKCε-specific activator, ψεRACK or TAT-peptide control (KAI Pharmaceuticals, San Francisco, CA, USA) at a dose of 0.2 mg/kg, a neuroprotective concentration in vivo.[29] Brains were used for Western blotting, immunofluorescence, or RNA experiments.

Organotypic hippocampal cultured slice preparation

Hippocampal cultured slices were prepared as previously described.[14] Briefly, P9-13 Sprague Dawley pups were anesthetized (1 mg/kg ketamine), decapitated, and hippocampi were isolated and placed on a custom-made tissue chopper. Transverse slices (400 μm) were placed into 4°C Gey's Balanced salt solution. Slices with distinct and intact hippocampal morphology containing the dentate gyrus, CA3, and CA1 were plated onto 0.4-μm Millicell well inserts (Millipore, Billerica, MA, USA) in media containing 25% horse serum, 25% Hanks balanced salt solution (HBSS), and 50% minimal essential media, supplemented with 1 mM glutamine and 30 mM glucose. Media was changed one day following plating and subsequently twice a week. Experiments began 14 days after culturing. Slices were used for electrophysiology, Western blotting, or cell death experiments. Unless specified, all chemicals were purchased from Sigma-Aldrich (St. Louis, MO, USA).

Drug administration for hippocampal cultured slices

For PKCε-activation, slices were treated with 200 nM of ψεRACK[14] for 1 h and kept at 36°C. For experiments blocking TrkB, the specific TrkB inhibitor, ANA-12 (10 μM),[30] was administered 24 h prior to ψεRACK treatment. To determine the effect of blocking arc expression, 1 nM arc antisense oligodeoxynucleotide (arc AS ODN) or 1 nM scrambled control ODN (SC ODN) was added to each well 24 h prior to ψεRACK or TAT treatment. ODNs were prepared in PBS (pH 7.4). ODN sequences: arc AS ODN: 5′-GTCCAGCTCCATCTGCTCGC-3′; SC ODN: 5′-CGTGCACCTCTCGCAGCTTC-3′ the three outer most linkages contain phosphorothiate linkages (Midland Certified Reagent Company, Midland, TX, USA).[31–33] For experiments examining the role of GluR2 internalization, 10 μM of TAT-GluR2$_{3Y}$ (prevents GluR2 internalization) or TAT-GluR2$_{3A}$

(control) was added into the internal solution. Peptide sequences are as indicated in Ahmadian et al.:[34] TAT-GluR2$_{3Y}$ sequence N′ to C′: YGRKKRRQRRRYKE GYNVYG; TAT-GluR2$_{3A}$ sequence: YGRKKRRQ RRRAKEGANVAG (Anaspec, Freemont, CA, USA). Peptide was allowed to defuse into the cell for 10 min prior to recordings.

Oxygen and glucose deprivation

Slices were washed three times in glucose-free HBSS containing 1.26 mM $CaCl_2$ 5.37 mM KCl, 0.44 mM KH_2PO_3, 0.49 mM $MgCl_2$, 0.41 mM $MgSO_4$, 136.9 mM NaCl, 4.17 mM $NaHCO_3$, 0.34 mM Na_2HPO_4, and 30 mM sucrose. Slices were placed in fresh glucose-free media and moved into an airlock chamber (Coy Lab Products, Grass Lake MI, USA) flushed with 90% N_2/5%CO_2/5%H_2 gas (37°C) to remove oxygen. Following 35 min of oxygen and glucose deprivation (OGD), slices were returned to a 36°C normoxic incubator with fresh glucose containing media.[14,16]

Western blotting

Tissue was homogenized in RIPA buffer solution (pH 8.0) containing 150 mM NaCl, 1% NP-40, 0.5% sodium deoxycholate, 0.1% SDS, 50 mM Tris, supplemented with 1% protease antibodies (Sigma) and phosphatase inhibitor cocktails (Roche Molecular Systems Inc., Branchburg, NJ, USA). Lysates were centrifuged at 16,000 *g* for 15 min. Protein was concentration determined by Bio-Rad protein assay (Bio-Rad, Hercules, CA, USA). Protein samples (30 or 40 μg) were separated on a 10 or 12% SDS-PAGE gel then electrophoretically transferred onto nitrocellulose membranes (Bio-Rad). Blots were blocked in 5% milk in Tris-buffered saline with 1% tween then incubated overnight in primary antibody in 5% milk. Blots were washed then incubated for 1 h in horseradish peroxidase-conjugated anti-mouse or anti-rabbit secondary antibodies (Sigma). Blots were developed on film or using the VersaDoc 4000 MP (Bio-Rad). For blots imaged using the VersaDoc, each blot was imaged so that intensity of samples was within a linear range. Westerns were quantified using ImageJ. Antibodies used: actin (Sigma, 1:5000), BDNF (Santa Cruz Biotechnology, Santa Cruz, CA, USA,1:200), TrkB (Cell Signaling Technologies, Boston, MA, USA, 1:1000), phosphorylated TrkB (pTrkB) (Millipore, 1:1000), and arc (Santa Cruz, 1:200).

Immunofluorescence

Twenty-five-day-old Sprague Dawley rats were anesthetized, then perfused with saline followed by 4% paraformaldehyde in PBS and post-fixed overnight. Brains were removed, cryoprotected in a 20% sucrose solution for two days, frozen, then cryosectioned (30 μm). Coronal hippocampal sections were taken at −3.8 mm bregma. Sections were washed in PBS with 0.8% triton X-100 (PBST) three times and blocked overnight at 4°C in 10% goat serum in PBST. Sections were then washed three times in PBST and incubated with 1:500 NeuN (Millipore) and 1:50 Arc (H-300 Santa Cruz) in PBS for 72 h. Slices were then washed in PBS three times and secondary anti-mouse alexa fluor 568 (Life Technologies, Grand Island, NY, USA, 1:500) and anti-rabbit hilyte fluor 488 (AnaSpec, 1:500) were applied for 2 h at room temperature. Slices were mounted using Prolong Antifade reagent (Molecular Probes, Carlsbad, CA, USA) and visualized using a Zeiss LSM 700 Confocal microscope at 63X magnification.

Real-time PCR analysis

RNA was extracted from the hippocampi of 25-day-old rats 48 h following an i.p. injection (0.2 mg/kg) of ψεRACK or TAT control. RNA was extracted as described.[35,36] Briefly, hippocampi were homogenized in TRIzol (Life Technologies, Carlsbad, CA, USA) followed by column RNA extraction using the RNeasy Mini kit (Qiagen, Hilden, Germany). To remove contaminating DNA, DNase digestion (Qiagen) was performed during the RNA extraction procedure. RNA (1 μg) was then reverse transcribed using the qScript cDNA synthesis kit (Quantabio, Beverly, MA, USA). cDNA was then diluted 1:5 and used as a template for real-time PCR analysis using *Power* SYBR green PCR Master Mix (Life Technologies). The relative expression was calculated based on the ΔΔCt method with β-actin (ACTB) used as an endogenous control. Three technical replicates were performed for each qRT-PCR reaction. The target mRNA for rat genes was obtained from *Ensembl* and primers were designed to amplify a product size between 80 and 120 bases and to span an exon junction to avoid the amplification of any residual DNA contaminants. Primer sequences (from 5′to 3′): Arc forward: TTCAGAGCCAGGAGAACGAC; Arc reverse: CAGGCAGCTTCAAGAGAGGA; Actin forward: GTCTTCCCCTCCATCGTG; Actin reverse: AGGGTCAGGATGCCTCTCTT; GluR1 forward: GAAGCAGGCTCCACTAAGGA; GluR1 reverse: ACGGATGGTTCTGCAGACTT; GluR2 forward: ATGGGACAAGTTCGCATACC; GluR2 reverse: ACCTGCCACTTCTTCTCTGC; GluR3 forward: GGGTGCCATTCTGAGTCTTC; GluR3 reverse: CTGCTGCCTCCATAATTGCT; GluR4 forward: TGAGCCTCCTGGATCACTATG; GluR4 reverse: CCATCCATTTTGTCCTGCTT.

Propidium iodide measurements of cell death in organotypic slices

Slices were incubated in media supplemented with 2 μg/mL propidium iodide (PI). PI fluorescence was measured at four time points: (1) prior to ODN administration, (2) prior to OGD, (3) 24 h after OGD, and (4) 24 h following an hour application of 500 nM NMDA (to cause maximal neuronal death). Images of the CA1 region were captured with an Olympus IX50 fluorescent microscope using SPOT CCD camera and software and quantified with ImageJ. OGD-mediated cell death was quantified as % PI fluorescence expressed as [(post OGD – prior to OGD)/(post NMDA – prior to OGD)] × 100.[37] Toxicity of ODN treatment was quantified as % PI fluorescence expressed as [(prior to OGD – prior to ODN)/(post NMDA)].

AMPA miniature excitatory postsynaptic current measurements

Whole-cell voltage clamp was used to record miniature excitatory postsynaptic (mEPSC) AMPAR-mediated currents. Forty-eight hours after treatment with TAT or ψεRACK in the presence or absence of SC or arc AS ODNs, organotypic hippocampal cultured slices were submerged in an external solution containing 150 mM NaCl, 3.0 mM KCl, 2.5 mM $CaCl_2$, 1.3 mM $MgSO_4$, 1.3 mM $NaPO_4$, 25 mM $NaHCO_3$, 10 mM glucose, and bubbled with 95%O_2/5%CO_2. Bicuculline (10 μM), D-(-)-2-amino-5-phosphonopentanoic acid (20 μM, APV) and tetrodotoxin (1 μM, TTX) were added to inhibit GABA receptor currents, NMDA receptor currents, and spontaneous EPSCs, respectively. The internal solution of the pipette contained 122.5 mM $CsMSO_4$, 10 mM CsCl, 10 mM HEPES, 10 mM EGTA, 10 mM glucose, 8 mM NaCl, 2 mM MgATP, 1 mM $CaCl_2$, and 0.3 mM NaGTP at pH 7.4 (with NaOH) and 317 mOsm. For experiments examining the contribution of GluR2 endocytosis, TAT-$GluR2_{3Y}$ (GluR2 endocytosis inhibitor) or TAT-$GluR2_{3A}$ (control) peptide was added into the internal solution. Pipettes (2-5 MΩ) were made from borosilicate glass capillaries (Word Precision Instruments, Sarasota, FL, USA). CA1 hippocampal pyramidal neurons were targeted and visualized using Alexa 488 dye. One cell was patched per slice equating to an n = 1. A GΩ seal was obtained followed by a whole cell configuration in voltage clamp mode. Access resistance was maintained under 20 MΩ and recordings that drifted more than 4 MΩ were discarded. Two minute gap-free recordings were obtained in current clamp mode using the program pCLAMP 9.0 (Molecular Devices, Silicon Valley, CA, USA). The first 100 miniature events over each gap-free recording for each cell were used for analysis of maximum amplitude, maximum amplitude distribution, and event frequency. If less than 100 events occurred, the total number of events in the recording were used. mEPSCs were selected using Clampfit event detection software with a custom made filter.

Anoxic depolarization

Organotypic slices were used to obtain whole cell recordings 48 h following treatment with TAT or ψεRACK in the presence or absence of SC or arc AS ODNs. Slices were in the same external solution described above excluding bicuculline and APV. The internal solution of the pipette contained 140 mM K^+-gluconate, 5 mM KCl, 10 mM HEPES, 10 mM EGTA, 2 mM $MgCl_2$, 2 mM MgATP, and 0.5 mM NaGTP (pH 7.33). For experiments with the TAT-$GluR2_{3Y}$ or TAT-$GluR2_{3A}$ peptides, peptides were added into the internal solution. CA1 hippocampal pyramidal neurons were targeted and visualized using Alexa 488 dye. One cell was patched per slice equating to an n = 1. Whole cell configuration and access resistance were maintained as described above. To initialize the OGD, the external perfusate was switched to a glucose free media (where sucrose replaces glucose) that was vigorously bubbled with a 95% N_2/5%CO_2 gas mixture. Latency until AD onset was marked as a rapid change from resting membrane potential.[38]

Statistical analysis

Results are expressed as means ± SEM. Student's *t*-test, one-way ANOVA with Bonferroni post-hoc analysis, linear regression, and Kolmogorov-Smirnov statistical tests were used as indicated. Significance denoted as $* = p < 0.05$, $** = p < 0.01$, and $*** = p < 0.005$. Statistical software SPSS version 21 was used. For Western blot experiment confirming knockdown of arc with arc AS ODN in organotypic hippocampal cultured slices, slices obtained from one animal were divided into two groups and treated with SC ODN or arc AS ODN. Twelve hippocampi slices from the same litter and same treatment were pooled for Western blot analysis for an n = 1. Healthy organotypic slices were selected randomly from each plate for each treatment group for all organotypic experiments. Researchers were appropriately blinded for both experimentation and analysis throughout the study. Sample sizes were selected depending upon prior experiments conducted by the lab and power analysis in order to detect an effect size of 0.8 using the program G*power 3.1. Data were reported in compliance with the ARRIVE guidelines.

Results

PKCε activation increases hippocampal BDNF expression and TrkB phosphorylation in vivo

PKCε-mediated preconditioning has previously been shown to confer neuroprotection after 48 hours.[16,20,39–41] Recently, our laboratory reported that BDNF protein expression increases following PKCε-activation in vitro[20] and previous reports have indicated that prolonged BDNF expression and TrkB activation robustly increase arc expression.[26] Therefore, we sought to examine the BDNF/TrkB signaling pathway at 6 (an early time point), 24 (an intermediate time point), and 48 (protective time point) h following PKCε activation. To test the hypothesis that PKCε activation increases BDNF expression and results in TrkB receptor activation in vivo, 25-day-old Sprague Dawley rats were administered ψεRACK (specific PKCε activator) or TAT control peptide (0.2 mg/kg; i.p.) and hippocampal expression of BDNF and pTrkB were measured 6, 24, and 48 h later via Western blot (Figure 1). Six hours following PKCε-activation with ψεRACK, BDNF

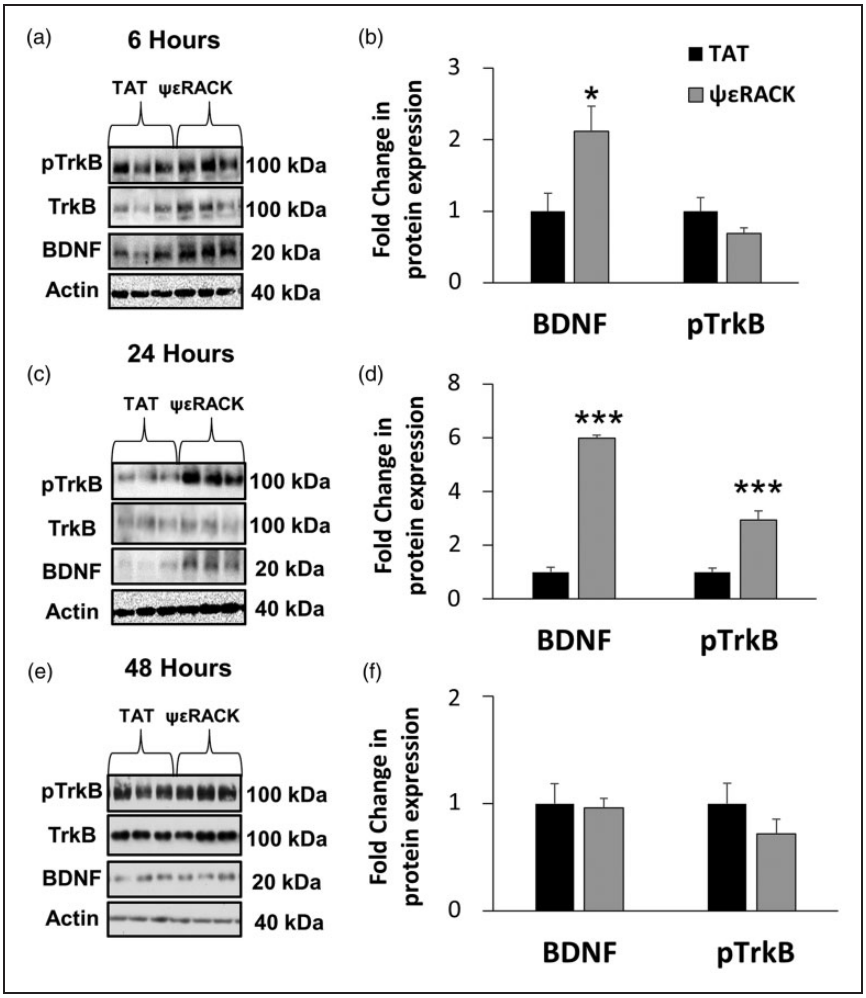

Figure 1. ΨεRACK administration increases BDNF protein levels and TrkB phosphorylation in the hippocampus *in vivo*. (a) Twenty-five-day old Sprague Dawley rats were injected i.p. with 0.2 mg/kg ψεRACK (specific PKCε activator) or TAT peptide control. Whole cell, hippocampal homogenates were obtained 6 (a–b), 24 (c–d), or 48 (e–f) h following treatment. BDNF expression normalized to actin and TrkB phosphorylation normalized to TrkB expression were quantified via Western blot. Samples collected from a single time point were run on the same blot. (a) Representative Western blot of BDNF, TrkB, pTrkB and actin 6 h post ψεRACK or TAT peptide injection. (b) Quantification of (a). BDNF levels were increased compared to a TAT peptide at 6 h following BDNF expression ($n = 4$, $p < 0.05$, Student's *t*-test). (c) Representative Western blot of BDNF, TrkB, pTrkB and actin 24 h post ψεRACK or TAT peptide injection. (d) Quantification of (c). At 24 h following ψεRACK injection, BDNF and pTrkB levels were increased compared to TAT ($n = 4$, $p < 0.005$, $p < 0.005$, respectively, Student's *t*-test). (e) Representative Western blot of BDNF, TrkB, pTrkB and actin 48 hours post ψεRACK or TAT peptide injection. (f) Quantification of (e). There were no observed differences in BDNF expression or TrkB phosphorylation at 48 h.

expression was significantly increased 2.12 ± 0.35-fold compared to the TAT peptide control ($n = 4$, $p < 0.05$, Student's t-test); however, TrkB phosphorylation (pTrkB) was not different from the TAT controls at this time point ($n = 4$, $p < 0.05$, Student's t-test) (Figure 1(a) and (b)). Twenty-four hours following ψεRACK administration, BDNF expression was increased 5.99 ± 0.11-fold compared to TAT peptide ($n = 4$, $p < 0.005$, Student's t-test), and pTrkB was increased 2.94 ± 0.32-fold compared to TAT peptide ($n = 4$, $p < 0.005$, Student's t-test) (Figure 1(c) and (d)). Forty-eight hours following administration of ψεRACK or the TAT peptide, there was no observed differences between groups for BDNF protein expression ($n = 5$, $p = 0.85$, Student's t-test) or pTrkB ($n = 5$, $p = 0.26$, Student's t-test) (Figure 1(e) and (f)).

PKCε increases CA1 hippocampal arc expression in vivo

It is well established that BDNF expression increases the expression of arc.[22–26] As we determined that PKCε activation enhances BDNF expression and downstream signaling, we hypothesized that PKCε activation increases hippocampal arc expression in vivo. To test this hypothesis, 0.2 mg/kg of ψεRACK (specific PKCε activator) or a TAT control peptide was injected in 25-day-old Sprague Dawley rats. Forty eight hours later, tissue was collected to evaluate hippocampal arc protein expression (Figure 2(a) and (b)), mRNA expression (Figure 2(c)), and CA1 protein localization (Figure 2(d) to (i)). ΨεRACK administration increased arc expression 1.91 ± 0.22-fold compared to TAT peptide treated control ($n = 9$, $p < 0.005$, Student's t-test) (Figure 2(a) and (b)) and increased arc mRNA expression to 143.97 ± 7.68 % of TAT ($n = 10$, $p < 0.05$, Student's t-test) (Figure 2(c)). CA1 pyramidal cells were probed for the neuronal marker NeuN (Figure 2(d) and (e)) and arc (Figure 2(f) and (g)). Qualitative immunofluorescence shows that PKCε activation with ψεRACK increases the localization of arc expression into cell bodies of CA1 pyramidal neurons (Figure 2(h) and (i)).

PKCε activation decreases GluR receptor mRNA expression in vivo

Arc protein expression has previously been linked to GluR mRNA expression.[42] We examined mRNA expression of four glutamate receptor subunits (GluR1, GluR2, GluR3, and GluR4) 48 h following ψεRACK or TAT injection in vivo (Figure 2(j)). mRNA expression of GluR1 after ψεRACK injection was 83.67 ± 7.31 % of TAT control but this difference was not statistically significant ($n = 10$, $p = 0.07$, Student's t-test). ΨεRACK injection decreased GluR2 mRNA expression to $79.30 \pm 5.00\%$ of TAT control ($n = 10$, $p < 0.05$, Student's t-test). GluR3 and GluR4 mRNA expression were not significantly different between the ψεRACK treatment and TAT peptide control groups ($p = 0.17$ and $p = 0.95$ respectively, Student's t-test). Linear regressions between arc mRNA expression and mRNA expression of each GluR subunit for all animals in both groups ($N = 19$) were performed to better elucidate the relationship between the two factors. GluR1 expression is inversely related to arc expression (Figure 2(k)) ($N = 19$, $r = -0.52$, $p < 0.05$, linear regression). Additionally, GluR2 is inversely correlated with arc mRNA expression (Figure 2(l)) ($N = 19$, $r = -0.53$, $p < 0.05$, linear regression). There were no observed relationships between arc mRNA expression and either GluR3 mRNA (Figure 2(m)) ($N = 19\, r = -0.33$, $p = 0.17$, linear regression) or GluR4 mRNA expression (Figure 2(n)) ($N = 19$, $r = 0.017$, $p = 0.95$, linear regression).

PKCε-mediated arc expression decreases AMPAR miniature excitatory postsynaptic current maximum amplitudes in vitro

A well characterized function of arc is to alter the number of cell surface AMPARs through increasing endocytosis[27] and regulating AMPAR transcription[42] leading to a decrease in AMPAR-mediated mEPSC amplitude. As our previous results show that PKCε activation enhances arc expression and decreases AMPAR subunit transcription, we wanted to examine the effect of PKCε activation on AMPAR currents. To determine the contribution of arc, arc protein expression was inhibited in organotypic slices with arc AS ODNs, a well characterized technique to inhibit arc expression;[31] scrambled control oligodeoxynucleotides (SC ODNs) served as experimental controls. Arc AS ODNs decreased arc protein expression in organotypic hippocampal cultured slices to $56.84 \pm 24.08\%$ of SC ODN (Figure 3(a) and (b)) ($n = 3$, $p < 0.05$, paired t-test) which is a similar decrease in protein expression to what others have reported when utilizing these ODNs.[31,33,43] Then, we tested the hypothesis that PKCε activation reduces AMPAR-mediated currents through an arc-dependent pathway. Forty-eight hours following a 1 h ψεRACK or TAT (200 nM) treatment, AMPAR mEPSCs were recorded in organotypic hippocampal cultured slices (Figure 3(c) and (d)). The culture media of a subset of slices was maintained with SC or arc AS ODNs beginning 24 h prior to the ψεRACK treatment to determine the contribution of arc expression in modulation of AMPAR mEPSCs after PKCε activation (Figure 3(c) and (d)). Treatment of

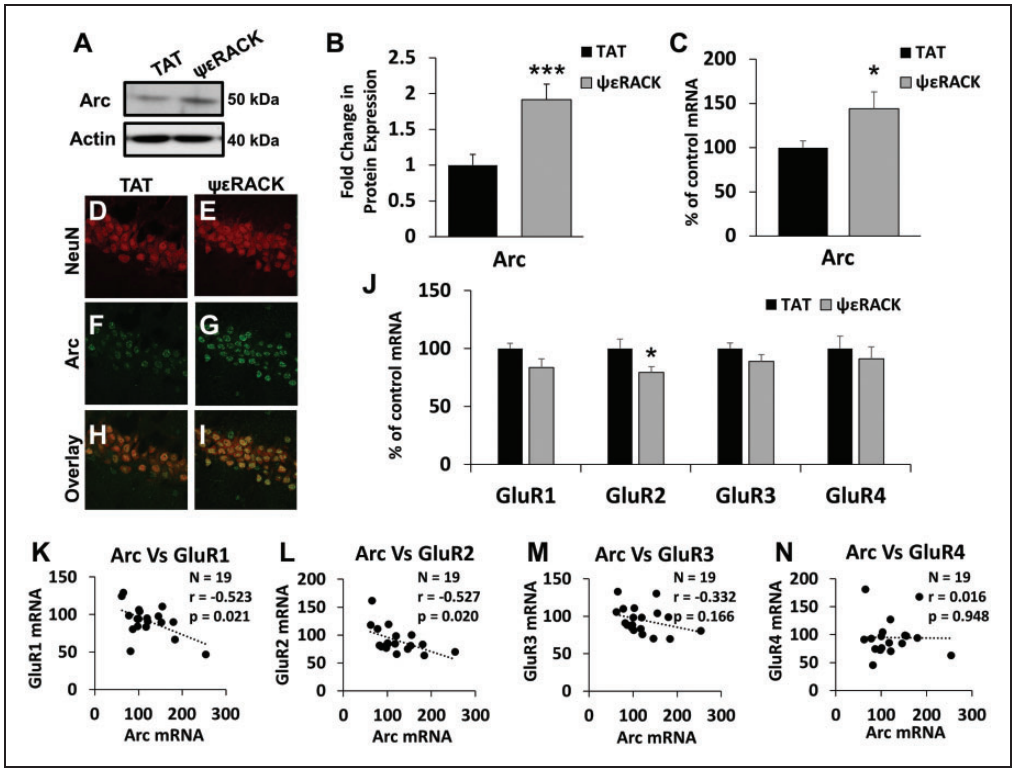

Figure 2. ΨεRACK administration increases arc protein expression in CA1 neurons in vivo. (a) Twenty-five-day-old Sprague Dawley rats were injected i.p. with 0.2 mg/kg ψεRACK (specific PKCε activator) or TAT peptide control. Whole cell hippocampal homogenates were obtained 48 h following administration and activity-regulated cytoskeleton-associated protein (arc) levels were quantified via Western blot. (a) Representative Western blot showing enhanced arc expression with ψεRACK treatment. (b) Quantification of western blot described in (a). Arc protein levels were elevated compared to a TAT peptide treated control ($n = 9$, $p < 0.005$, Student's *t*-test). (c) 48 h following ψεRACK injection, arc mRNA expression levels increase to 143.97 ± 19.32 % of TAT control mRNA expression levels ($n = 10$ TAT and $n = 9$ ψεRACK, $p < 0.05$, Student's *t*-test). (d–i) Immunofluorescence images obtained 48 h following administration of 0.2 mg/kg ψεRACK. Sections were stained for NeuN (red) and arc (green) protein ($n = 4$). A visual increase in somatic arc protein was observed in CA1 pyramidal neurons. (j) GluR2 mRNA expression was decreased to 79.23 ± 5.00 % of TAT control ($n = 10$, $p < 0.05$, Student's *t*-test) 48 h following ψεRACK injection and GluR1 mRNA expression was trending down to 83.67 ± 7.31 % of TAT control ($n = 10$, $p = 0.07$, Student's *t*-test). (k–n) Arc mRNA expression is increased and GluR receptor subunit mRNA expression is decreased 48 h following in vivo injection of the PKCε-activator ψεRACK. Linear regression analyses were run to determine the relationship between arc mRNA expression and specific GluR subunit expression. There was a relationship between arc mRNA expression and GluR1 mRNA expression ($N = 19$, $r = -0.52$, $p < 0.05$, linear regression), and arc mRNA expression and GluR2 mRNA expression ($N = 19$, $r = -0.53$, $p < 0.05$, linear regression). There was no relationship observed between arc and GLuR3 mRNA expression ($N = 19$, $r = -0.33$, $p = 0.116$, linear regression) or arc and GluR4 arc mRNA expression ($N = 19$, $r = 0.016$, $p = 0.95$ linear regression).

organotypic slices with ψεRACK decreased the average maximum AMPAR-mediated mEPSCs amplitude to 12.75 ± 0.35 pA as compared to 14.80 ± 0.39 pA in TAT control-treated slices ($n = 20$, $p < 0.05$, one way ANOVA, Bonferroni post-hoc) (Figure 3(e)). The ψεRACK + SC ODN treatment similarly decreased average AMPAR-mediated mEPSC maximum amplitude to 12.47 ± 0.49 pA, as compared to the TAT control ($n = 20$, $p < 0.01$, one way ANOVA, Bonferroni-post hoc) (Figure 3(e)). However, this change in mEPSC amplitude was lost with the ψεRACK + arc AS ODN treatment as there was no observed change in mEPSC amplitude when compared to the TAT peptide ($n = 20$, $p = 0.63$, one way ANOVA, Bonferroni-post hoc) (Figure 3(e)). These data show that PKCε activation reduces AMPAR-mediated currents, an effect that is dependent on arc expression. There were no statistically significant changes in event frequency overall or between any of the groups ($n = 20$, $p = 0.29$, one way ANOVA, Bonferroni post hoc) (Figure 3(f)).

In addition to decreasing the average maximum mEPSC amplitude, the distribution of the maximum amplitudes for AMPAR-mediated mEPSCs was shifted towards smaller amplitude responses for the ψεRACK-treated group compared to TAT peptide controls ($n = 1853$ and $n = 1905$ respectively, $p < 0.005$,

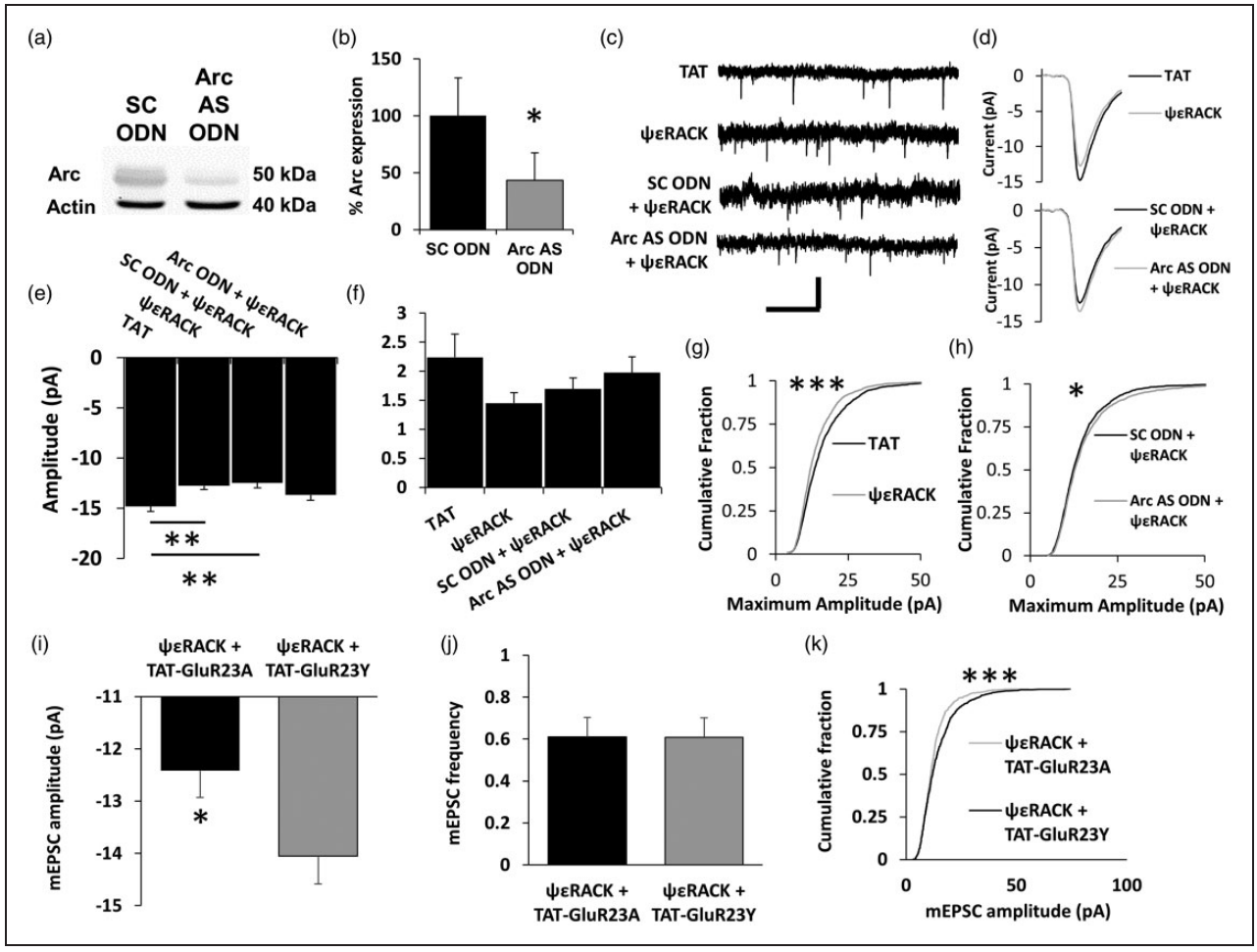

Figure 3. Inhibition of arc blocks PKCε-dependent AMPAR mEPSC amplitude changes. (a) Western blot of arc expression in organotypic hippocampal cultured slices treated with arc antisense oligodeoxynucleotide (arc AS ODN, 1 nM) or a scrambled control oligodeoxynucleotide (SC ODN, 1 nM) for 24 h. (b) Quantification of A; arc protein expression is decreased following 24 h of arc AS ODN treatment compared to scrambled control (n = 3, $p < 0.05$, paired *t*-test). Inhibition of arc blocks PKCε-dependent AMPAR mEPSC amplitude changes. (c) Organotypic hippocampal cultured slices were treated with arc AS ODN or SC ODN for 24 h prior to a 1 h treatment with TAT (200 nM) or ψεRACK (200 nM). In groups treated with arc AS ODN or SC ODN, ODNs were maintained in culture for the following 48 h. AMPAR-mediated mEPSCs were measured in the presence tetrodotoxin (TTX, 1 μM) bicuculline (10 μM), and APV (20 μM). Typical mEPSC tracings observed. (d) Average tracing of all mEPSCs recorded for each group. (e) Maximum mEPSC amplitude of TAT, ψεRACK, ψεRACK + arc AS ODN, and ψεRACK + SC ODN-treated groups. Following administration of ψεRACK, the maximum amplitude was decreased as compared to a TAT control group (n = 20 slices, $p < 0.05$, one-way ANOVA, Bonferroni post hoc). ΨεRACK + SC ODN also decreased the maximum mEPSC amplitude as compared to a TAT control group (n = 20 slices, $p < 0.01$, one-way ANOVA, one-way Bonferroni post hoc). The ψεRACK + arc AS ODN showed no decrease in maximum amplitude observed as compared to the TAT group (n = 20 slices, $p > 0.05$, ANOVA, Bonferroni). (f) There were no significant changes in event frequency between any of the groups (n = 20, $p > 0.05$, one-way ANOVA, Bonferroni post hoc). (g–h) Cumulative fraction plots examining the changes of the distribution for all of the events for the TAT (n = 1905), ψεRACK (n = 1853), ψεRACK + SC ODN (n = 1964), and ψεRACK + arc AS ODN (n = 1977) groups. The distribution of amplitude of total mEPSCs was shifted towards smaller maximum amplitudes in slices treated with ψεRACK compared to a TAT control ($p < 0.005$, Kolmogorov–Smirnov Test). The presence of the arc AS ODN increased the maximum amplitude as compared to ψεRACK + SC ODN ($p < 0.05$, Kolmogorov–Smirnov Test). (i) PKCε-mediated changes in mEPSC amplitude and latency until AD are blocked by inhibiting GluR2 internalization. Application of TAT-GluR2$_{3Y}$ peptide within the internal solution blocked the PKCε-mediated reduction in mEPSC amplitude (n = 12, $p < 0.05$, Student's *t*-test). (j) mEPSC frequency was unchanged between the two groups, indicating that TAT-GluR2$_{3Y}$ peptide application had no effect on mEPSC frequency. (k) ΨεRACK + TAT-GluR2$_{3Y}$ group also had shifted distribution towards larger responses compared to the ψεRACK + TAT-GluR2$_{3A}$ group (n = 762 and 761 respectively, $p < 0.005$, Kolmogorov–Smirnov Test).

Kolmogorov–Smirnov test) (Figure 3(g)). This effect is also dependent upon arc expression as ψεRACK + arc AS ODN treatment shifted the distribution of the maximum amplitude for total events measured towards larger responses when compared to the ψεRACK + SC ODN controls (n = 1977 and n = 1964 respectively, $p < 0.05$, Kolmogorov–Smirnov test) (Figure 3(h)).

PKCε-mediated reduction in AMPAR mEPSCs is blocked by inhibiting GluR2 internalization

Arc is known to induce internalization of surface AMPARs.[27,42] To directly test if this role of arc was important in the PKCε-mediated reduction of AMPAR mEPSC amplitude, we utilized a peptide, $GluR2_{3Y}$, which prevents GluR2 internalization. $GluR2_{3Y}$ has previously been shown to impair arc-dependent AMPAR internalization.[44] This peptide mimics and blocks the phosphorylation of Y869, Y873, Y879, which are necessary for subunit internalization.[34] AMPAR mEPSCs were recorded in organotypic slices 48 h after treatment ψεRACK and either $GluR2_{3Y}$ (GluR2 internalization inhibitor) or $GluR2_{3A}$ (control) peptide was added to the internal solution. While ψεRACK application decreased AMPAR mEPSC amplitudes (Figure 3(c) to (e)), this decrease was impaired when GluR internalization was blocked: ψεRACK + $GluR2_{3Y}$ maximum AMPAR mEPSCs was -14.05 ± 0.54 pA as compared to -12.42 ± 0.51 pA observed in a ψεRACK + control $GluR2_{3A}$ peptide (n = 12, $p < 0.05$, Student's *t*-test) (Figure 3(i)). The average maximum AMPAR mEPSC amplitude in the ψεRACK + control $GluR2_{3A}$ treatment was similar to ψεRACK treatment alone, suggesting control peptide had no effect. mEPSC frequency was unchanged by ψεRACK + $GluR2_{3Y}$ peptide compared to the control ψεRACK + $GluR2_{3A}$ group (Figure 3(j)). Additionally, the distribution of mEPSC maximum amplitude responses was shifted towards larger responses in the ψεRACK + $GluR2_{3Y}$ peptide compared to the ψεRACK + $GluR2_{3A}$ control group (n = 761, 762 respectively, $p < 0.005$, Kolmgorov–Smirnov test) (Figure 3(k)).

PKCε-mediated arc expression delays the latency until anoxic depolarization in organotypic hippocampal cultured slices through a GluR2-dependent process

Long lasting AD is a catastrophic process often resulting in cell death.[45] A previous study showed that direct pharmacological inhibition of AMPARs can increase the latency until AD in acute hippocampal slices.[38] Decreasing postsynaptic AMPARs through increased arc expression may lead to a similar delay in AD. To test the hypothesis that PKCε activation would cause an arc-dependent increase in latency until AD, we recorded membrane potential in CA1 neurons treated with TAT, ψεRACK, ψεRACK + SC ODN, or ψεRACK + arc AS ODN (as described above) during an irreversible OGD (Figure 4(a) and (b)). Forty-eight hours following TAT or ψεRACK treatment, latency until AD was increased from 29.27 ± 3.6 min in TAT-treated slices to 50.77 ± 5.08 min after ψεRACK treatment ($p < 0.05$) and 52.73 ± 6.78 min after ψεRACK + SC ODN treatment ($p < 0.05$) (n = 13–15, Bonferroni post hoc) (Figure 4(c)). Enhanced latency after ψεRACK treatment was reduced when arc expression was inhibited; latency until AD was 39.5 ± 5.63 min for the ψεRACK + arc AS ODN group, not significantly different from the TAT control (n = 14, $p = 1.000$, one way ANOVA, Bonferroni post-hoc). These are novel data that PKCε activation enhances latency till AD through an arc-dependent mechanism. Additionally, we hypothesized that blocking GluR2 internalization with application of the $GluR2_{3Y}$ peptide would reverse the ψεRACK-dependent increase in latency until AD. Blocking GluR2 internalization by application of the $GluR2_{3Y}$ peptide following ψεRACK treatment reduced latency until AD to 22.3 ± 5.17 min compared to 54.5 ± 8.40 min in the ψεRACK + $GluR2_{3A}$ control group (n = 6, $p < 0.005$, Student's *t*-test) (Figure 4(d)).

PKCε-dependent arc expression is necessary for neuroprotection against oxygen and glucose deprivation in vitro

Our previous experiments suggest a novel mechanism of PKCε-mediated neuroprotection where application of ψεRACK enhanced BDNF signaling resulting in increased arc expression, reduced AMPAR mEPSCs, and enhanced latency until AD. Therefore, we tested the role of BDNF/TrkB signaling in conferring neuroprotection in organotypic slices. We hypothesized that PKCε-dependent activation of TrkB was necessary for conferring neuroprotection against a lethal OGD. Organotypic hippocampal cultured slices were subject to 1 h treatment of ψεRACK or TAT control and subject to a lethal OGD 48 h later. Media in a subset of slices was supplemented with a TrkB specific inhibitor, ANA-12 (10 μM), or DMSO control (0.01%) beginning 24 h prior to the 1 h administration of ψεRACK or TAT control peptide (Figure 4(e)). Inhibiting TrkB with ANA-12 impaired the protective effect of ψεRACK increasing CA1 cell death from $20.80 \pm 6.20\%$ with ψεRACK + DMSO control treatment to $60.67 \pm 12.11\%$ ψεRACK + ANA-12 (n = 7, $p < 0.005$, one way ANOVA, Bonferroni post hoc) (Figure 4(e)).

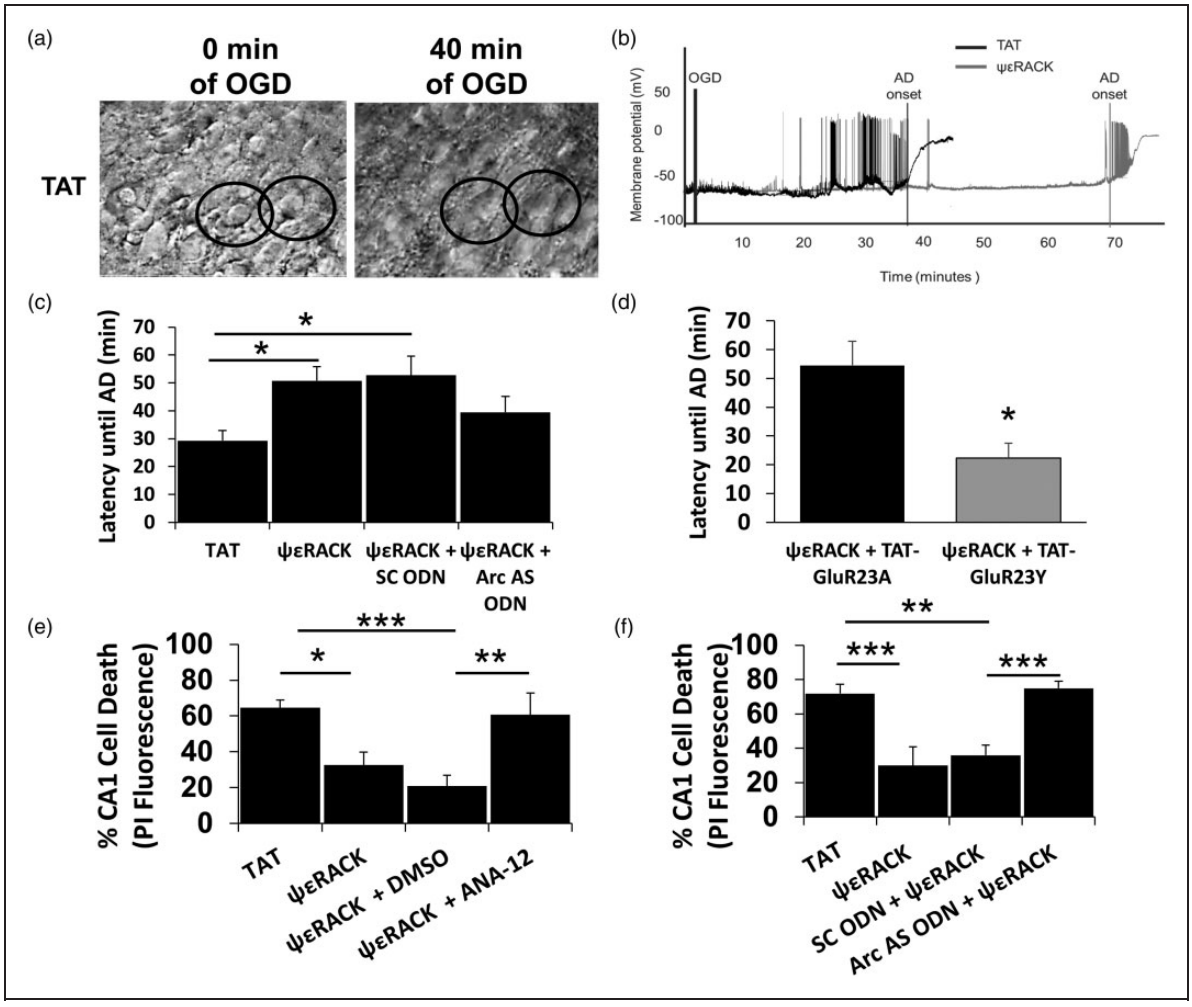

Figure 4. Inhibition of arc and GluR2-internalization impairs PKCε-dependent increases in latency until AD and TrkB/arc signaling is necessary for PKCε-mediated neuroprotection. (a) Example images of TAT treated organotypic slices that have undergone 0 and 40 min of anoxic depolarization (AD). Two cells that have undergone significant swelling during the AD are circled. (b) Example membrane potential changes over time for organotypic hippocampal cultured slices during OGD that were treated with TAT or ψεRACK for 1 h 48 h prior to OGD. The sharp rise in membrane potential illustrates the initiation of AD. (c) Latency until AD was increased in the ψεRACK and ψεRACK + SC ODN groups compared to TAT ($n = 13–15$, $p < 0.05$, $p < 0.05$ respectively, one-way ANOVA, Bonferroni post hoc). Latency until AD for the ψεRACK + arc AS ODN group was not significantly different from the TAT control ($n = 14$, $p = 1.000$, one-way ANOVA, Bonferroni post hoc). (d) TAT-GluR2$_{3Y}$ application additionally blocked a PKCε-dependent increase in latency until AD ($n = 6$, $p < 0.005$, Student's *t*-test). (e) The TrkB pathway was inhibited in organotypic hippocampal cultured slices using the specific inhibitor ANA-12 (10 μM) 24 h prior to, during 1 h administration of ψεRACK (200 nM), and for 48 h prior to a lethal OGD. Inhibition of TrkB impaired ψεRACK neuroprotection compared to its ψεRACK + DMSO control ($n = 7–8$, $p < 0.005$, one-way ANOVA, Bonferroni post-hoc). (f) Organotypic hippocampal cultured slices were treated with TAT peptide (200 nM), ψεRACK (200 nM), arc AS ODN + ψεRACK, or SC ODN + ψεRACK. Cell death in the CA1 region was observed 24 h following the lethal OGD using a 2 μg/ml propidium iodide (PI). ΨεRACK administration protected slices from a lethal OGD, reducing PI fluorescence as compared to TAT control ($n = 6$ $p < 0.005$, one way ANOVA, Bonferroni post hoc). Inhibition of arc with an arc AS ODN impaired ψεRACK-dependent neuroprotection against a lethal OGD compared to SC ODN + ψεRACK treated group ($n = 6$, $p < 0.005$, one way ANOVA, Bonferroni post hoc).

We examined the necessity of enhanced arc expression to confer neuroprotection after PKCε activation. We treated organotypic slices with TAT, ψεRACK, ψεRACK + SC ODN, or ψεRACK + arc AS ODN. ΨεRACK protected slices from lethal OGD 48 h later, reducing cell death from $71.89 \pm 5.33\%$ in the TAT control to $29.91 \pm 10.92\%$ in the ψεRACK-treated slices ($n = 6$, $p < 0.005$, one way ANOVA, Bonferroni post hoc) (Figure 4(f)). The ψεRACK + SC ODN treatment also protected against a lethal OGD as only $35.91 \pm 5.97\%$ CA1 cell death was observed. In comparison, the ψεRACK + arc AS ODN abolished the

protective effect of ψεRACK treatment with 74.93 ± 4.24% CA1 cell death (n = 6, $p < 0.005$, one way ANOVA, Bonferroni post-hoc) (Figure 4(f)). The enhanced cell death in the arc AS ODN-treated group was not due to toxic effects of the peptide. None of the treatments (TAT, ψεRACK, ψεRACK + SC ODN, and ψεRACK + arc AS ODN) had any acute effect on cell death resulting in changes of −1.16 ± 2.73, 4.33 ± 1.54, 3.66 ± 2.09, and −1.20 ± 2.53% of maximal CA1 PI fluorescence respectively (n = 6, $p > 0.05$, one way ANOVA, Bonferroni post hoc).

Discussion

Here, we describe a novel mechanism whereby a novel isozyme of protein kinase C (i.e. PKCε) is involved in modulation of the BDNF/TrkB signaling cascade (Figure 1), which leads to enhanced arc expression (Figure 2). Arc expression, in turn, is necessary to alter AMPAR subunit expression (Figure 2) and promote AMPAR internalization (Figure 3). AMPAR internalization then delays latency until AD during OGD conferring neuroprotection (Figure 4). This arc-dependent shift in AMPAR-mediated currents provides a novel mechanism by which PKCε-activation mediates neuroprotection against excitotoxic injury through delaying latency until AD (Figure 5), but also implicates PKCε in synaptic regulation of the master regulator arc, which may have other physiological responses during normal synaptic function.

The function of decreasing synaptic AMPAR current is only part of a complex adaptive response triggered by PKCε activation. The signaling cascades activated by PKCε are multifaceted and may confer neuroprotection by modifications in mitochondria and at the synapse.[16,20,39–41] Thus, our result that inhibition of arc expression completely abolished the neuroprotective effect of PKCε activation was initially unexpected. Glutamatergic synaptic activity can consume 13% to 34% of the ATP stores within a cell.[46] Importantly, AD results from the failure of tissue ATP generation to match utilization.[47] Decreasing AMPAR glutamatergic signaling may allow for a cell to maintain ATP levels for longer periods, thereby delaying latency until

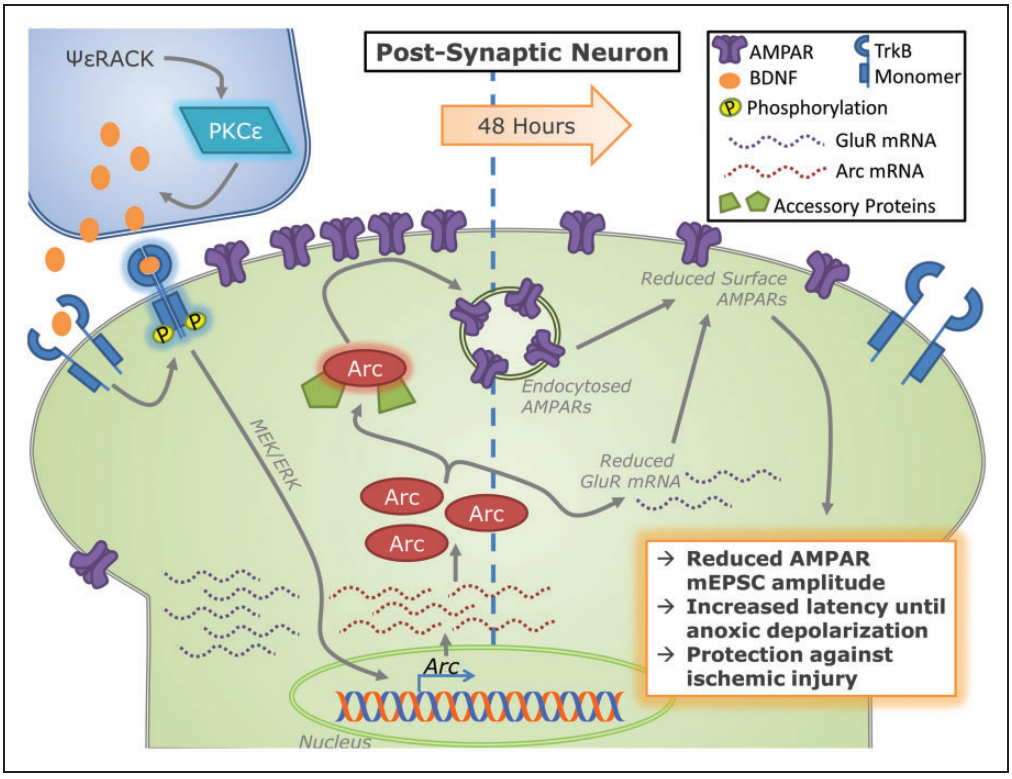

Figure 5. Mechanism of excitatory synaptic changes involved in PKCε-mediated preconditioning. Isoform specific activation of PKCε with ψεRACK enhances BDNF expression. BDNF activation of TrkB receptors enhances the transcription and expression of arc through a MEK/ERK dependent pathway.[22–26] Arc, in conjunction with accessory proteins, promotes AMPAR endocytosis[27] and decreases the mRNA expression of AMPAR subunits. Together, these changes result in the reduction of surface AMPAR abundance and consequentially AMPAR-mediated mEPSC amplitude 48 h later. A reduction in post-synaptic AMPARs increases the latency until anoxic depolarization providing tolerance to ischemic injury.

AD and providing neuroprotection. Activation of PKCε has previously been implicated in modulating GABAergic activity at the synapse which also may further contribute to decreasing the rate of ATP depletion through dampening of excitatory signaling. Two days following an hour ψεRACK treatment, there was an increase in GABA miniature inhibitory postsynaptic currents (mIPSC) and that enhanced GABAergic activity was necessary for neuroprotection.[16] Additionally, the ability of PKCε activation to increase mitochondrial efficiency may play an important role in determining latency until AD, as energy production through glycolysis and oxidative phosphorylation can extend latency until AD.[48] Together, PKCε-mediated changes to synaptic signaling and metabolic efficiency play an important role in maintaining ATP levels, which collectively play an important role in delaying the onset of AD.

PKCs can also modulate excitatory neurotransmission through the direct phosphorylation of AMPARs. The role of PKCs in regulating synaptic currents and receptor trafficking is more ambiguous due to the complex interplay between phosphorylation sites on the AMPARs as well as the surrounding synaptic machinery (for review, see Henley et al.[49]). Phosphorylation of serine 816 and serine 818 on the GluR1 subunit following pan-PKC activation by phorbol-esters can lead to immediate insertion of AMPARs into a synapse and play a critical role in the generation of long-term potentiation (LTP).[50,51] Both PKCα and PKCγ have been implicated as kinases involved in the phosphorylation of these sites.[51] In contrast to GluR1, phosphorylation of the GluR2 tyrosine sites Y869, Y873, Y879 can lead to endocytosis of AMPARs present on the cell surface,[34] indicating a role for an active endocytotic process. Previous publications have linked this active endocytosis process to arc expression.[44] However, no previous studies show that this process is linked to conventional or novel PKCs, or that it is necessary for modifying latency until AD.

Our novel finding that a decrease in AMPAR current is neuroprotective is consistent with previous publications that have indicated that AMPAR antagonism is neuroprotective against ischemic injury[52,53] and can increase latency until AD in the CA1 region.[38] Those studies used pharmacological treatments to inhibit AMPARs. Despite the potential for neuroprotection with AMPAR antagonism, clinical trials have failed due to a multitude of off target effects.[54] Results from our experiment utilizing the $GluR2_{3Y}$ peptide demonstrate for the first time that directly modulating AMPAR internalization can promote neuroprotection against ischemic injury and may have less adverse side-effects.

While activation of PKCε causes a 15% reduction in single cell AMPA mEPSC amplitude, it results in a 42% increase in latency until AD. Others have shown that small changes in AMPAR mEPSC amplitudes recorded in single cells underlie large changes in behavior and electrophysiological responses.[55,56] Ghosh et al.[55] found a 20% increase in AMPAR mEPSC amplitude was triggered by olfactory training tasks in the piriform cortex.[55] Also, Goforth et al.[56] found a mechanical injury caused a 17–25% change in AMPAR mEPSC amplitude – similar to the change found in the current study. This small percent change in AMPAR mEPSC amplitude and led to a drastic 20–42% reduction in frequency and amplitude of oscillations in small neuronal networks.[56] Through the use of the $GluR2_{3Y}$ peptide experiments, we were able to confirm the importance of the observed change in AMPAR content. By inhibiting PKCε-mediated internalization of GluR2 receptors, we prevented the reduction in mEPSC amplitude (Figure 3(i)) and determined that this change specifically was necessary for the PKCε-mediated increase latency until AD (Figure 4(d)). We found that there was no increase in latency until AD if the mEPSC amplitude change was blocked with the $GluR2_{3Y}$ peptide. To the best of our knowledge, modifying latency until AD time by reducing AMPAR receptor content has not previously been explored and is a novel aspect of this study. Most previous research on this topic has investigated the roll of receptor subtype changes, not focusing on overall post synaptic site receptor content, as changes in calcium permeability can also affect cell death following ischemic injury (see Liu et al.[57]). Along these lines, we observed a trending decrease in GluR1 mRNA expression and significant reduction in GluR2 mRNA expression. This is similar to a previous article indicating that nuclear arc expression decreased GluR1 expression.[42] With correlation analyses, we found a small, but significant inverse relationship between arc mRNA expression and mRNA expression of both GluR1 and GluR2. Future studies are needed to evaluate the importance of specific GluR subunit expression in PKCε-mediated preconditioning.

In addition to the BDNF/TrkB/MEK/ERK signaling cascade, PKCε-mediated increases in arc may be triggered by the phosphorylation of a related protein implicated in neuroprotection, cAMP-response element-binding protein (CREB). PKCε activation in vascular endothelium can promote CREB activation.[58] Additionally, Ying et al.[22] found that the MEK/ERK signaling activated by BDNF administration resulted in the phosphorylation of CREB in a pathway upstream of arc (mechanism reviewed in Bramham et al.[59]). Taken together, these studies suggest that CREB may be activated by PKCε activation and enhance arc expression. Additionally, CREB activation is upregulated at 6 and 24 h after estrogen preconditioning[60]

similar to the timing of BDNF upregulation found in the current study. Independent of arc activation, CREB-mediated preconditioning paradigms can regulate anti-apoptotic mechanisms via Bcl-2[61] and Bcl-xl[62] expression. While we cannot exclude the contribution of CREB activation in these alternative neuroprotective pathways or downstream of TrkB activation, we have found that arc is a necessary downstream mediator of PKCε preconditioning.

Arc is a well-characterized protein that is most commonly used as a marker of neuronal activity as its mRNA transcription is tightly coupled to neuronal activity and excitation.[31,63] A prior publication determined that following a global ischemic event, arc expression is minimal in a region susceptible to ischemic injury, the CA1, while its expression in a protected region, the dentate gyrus (DG), was preserved.[64] The difference between CA1 and DG could imply that the presence of arc in DG is able to protect it against an ischemic insult. We propose that decreasing AMPAR-mediated current amplitude through arc expression may contribute to this endogenous protection, but further studies would be warranted. To our knowledge, this is the first study reporting that PKCε mediates arc expression, that arc expression is necessary for PKCε-dependent neuroprotection, and that regulation of GluR2 internalization is important for modulating latency until anoxic depolarization.

Funding

The author(s) disclosed receipt of the following financial support for the research, authorship, and/or publication of this article: This work was supported by the National Institutes of Health grants NS45676, NS054147 and NS34773; and the Miami Evelyn F. McKnight Brain Institute.

Declaration of conflicting interests

The author(s) declared no potential conflicts of interest with respect to the research, authorship, and/or publication of this article.

Authors' contributions

CHC, CBW, and MAPP designed and planned experiments. CHC, HMSC, KCMB, NK, KBK, and MY conducted experiments and analysis. All the authors reviewed and wrote portions of the manuscript.

References

1. Go AS, Mozaffarian D, Roger VL, et al. Heart disease and stroke statistics – 2014 update: a report from the American Heart Association. *Circulation* 2014; 129: e28–e292.
2. McNally B, Robb R, Mehta M, et al. Out-of-hospital cardiac arrest surveillance – cardiac arrest registry to enhance survival (CARES), United States, October 1, 2005–December 31, 2010. *MMWR Surveill Summ* 2011; 60: 1–19.
3. Lim C, Alexander MP, LaFleche G, et al. The neurological and cognitive sequelae of cardiac arrest. *Neurology* 2004; 63: 1774–1778.
4. Richmond TS. Cerebral resuscitation after global brain ischemia: linking research to practice. *AACN Clin Issue* 1997; 8: 171–181.
5. Leao AA. Further observations on the spreading depression of activity in the cerebral cortex. *J Neurophysiol* 1947; 10: 409–414.
6. Hansen AJ, Hounsgaard J and Jahnsen H. Anoxia increases potassium conductance in hippocampal nerve cells. *Acta Phys Scand* 1982; 115: 301–310.
7. Czeh G, Aitken PG and Somjen GG. Membrane currents in CA1 pyramidal cells during spreading depression (SD) and SD-like hypoxic depolarization. *Brain Res* 1993; 632: 195–208.
8. Petito CK, Feldmann E, Pulsinelli WA and Plum F. Delayed hippocampal damage in humans following cardiorespiratory arrest. *Neurology* 1987; 37: 1281–6.
9. Horstmann A, Frisch S, Jentzsch RT, et al. Resuscitating the heart but losing the brain: brain atrophy in the aftermath of cardiac arrest. *Neurology* 2010; 74: 306–312.
10. Hickey RW, Akino M, Strausbaugh S, et al. Use of the Morris water maze and acoustic startle chamber to evaluate neurologic injury after asphyxial arrest in rats. *Pediatr Res* 1996; 39: 77–84.
11. Neigh GN, Glasper ER, Kofler J, et al. Cardiac arrest with cardiopulmonary resuscitation reduces dendritic spine density in CA1 pyramidal cells and selectively alters acquisition of spatial memory. *Eur J Neurosci* 2004; 20: 1865–1872.
12. Olsen GM, Scheel-Kruger J, Moller A, et al. Relation of spatial learning of rats in the Morris water maze task to the number of viable CA1 neurons following four-vessel occlusion. *Behav Neurosci* 1994; 108: 681–690.
13. Perez-Pinzon MA, Xu GP, Mumford PL, et al. Rapid ischemic preconditioning protects rats from cerebral anoxia/ischemia. *Adv Exp Med Biol* 1997; 428: 155–161.
14. Raval AP, Dave KR, Mochly-Rosen D, et al. Epsilon PKC is required for the induction of tolerance by ischemic and NMDA-mediated preconditioning in the organotypic hippocampal slice. *J Neurosci* 2003; 23: 384–391.
15. Sun X, Budas GR, Xu L, et al. Selective activation of protein kinase C in mitochondria is neuroprotective in vitro and reduces focal ischemic brain injury in mice. *J Neurosci Res* 2013; 91: 799–807.
16. DeFazio RA, Raval AP, Lin HW, et al. GABA synapses mediate neuroprotection after ischemic and epsilonPKC preconditioning in rat hippocampal slice cultures. *J Cereb Blood Flow Metab* 2009; 29: 375–384.
17. Xu C, Liu QY and Alkon DL. PKC activators enhance GABAergic neurotransmission and paired-pulse facilitation in hippocampal CA1 pyramidal neurons. *Neuroscience* 2014; 268: 75–86.
18. Sun MK, Hongpaisan J, Nelson TJ and Alkon DL. Poststroke neuronal rescue and synaptogenesis mediated

in vivo by protein kinase C in adult brains. *Proc Natl Acad Sci U S A* 2008; 105: 13620–13625.
19. Tan Z, Turner RC, Leon RL, et al. Bryostatin improves survival and reduces ischemic brain injury in aged rats after acute ischemic stroke. *Stroke* 2013; 44: 3490–3497.
20. Neumann JT, Thompson JW, Raval AP, et al. Increased BDNF protein expression after ischemic or PKC epsilon preconditioning promotes electrophysiologic changes that lead to neuroprotection. *J Cereb Blood Flow Metab* 2015; 35: 121–130.
21. Han BH and Holtzman DM. BDNF protects the neonatal brain from hypoxic-ischemic injury in vivo via the ERK pathway. *J Neurosci* 2000; 20: 5775–5781.
22. Ying SW, Futter M, Rosenblum K, et al. Brain-derived neurotrophic factor induces long-term potentiation in intact adult hippocampus: requirement for ERK activation coupled to CREB and upregulation of Arc synthesis. *J Neurosci* 2002; 22: 1532–1540.
23. Messaoudi E, Ying SW, Kanhema T, et al. Brain-derived neurotrophic factor triggers transcription-dependent, late phase long-term potentiation in vivo. *J Neurosci* 2002; 22: 7453–7461.
24. Messaoudi E, Kanhema T, Soule J, et al. Sustained Arc/Arg3.1 synthesis controls long-term potentiation consolidation through regulation of local actin polymerization in the dentate gyrus in vivo. *J Neurosci* 2007; 27: 10445–10455.
25. Yasuda M, Fukuchi M, Tabuchi A, et al. Robust stimulation of TrkB induces delayed increases in BDNF and Arc mRNA expressions in cultured rat cortical neurons via distinct mechanisms. *J Neurochem* 2007; 103: 626–636.
26. Ji Y, Lu Y, Yang F, et al. Acute and gradual increases in BDNF concentration elicit distinct signaling and functions in neurons. *Nat Neurosci* 2010; 13: 302–309.
27. Rial Verde EM, Lee-Osbourne J, Worley PF, et al. Increased expression of the immediate-early gene arc/arg3.1 reduces AMPA receptor-mediated synaptic transmission. *Neuron* 2006; 52: 461–474.
28. Irie Y, Yamagata K, Gan Y, et al. Molecular cloning and characterization of Amida, a novel protein which interacts with a neuron-specific immediate early gene product arc, contains novel nuclear localization signals, and causes cell death in cultured cells. *J Biol Chem* 2000; 275: 2647–2653.
29. Della-Morte D, Raval AP, Dave KR, et al. Post-ischemic activation of protein kinase C epsilon protects the hippocampus from cerebral ischemic injury via alterations in cerebral blood flow. *Neurosci Lett* 2011; 487: 158–162.
30. Cazorla M, Premont J, Mann A, et al. Identification of a low-molecular weight TrkB antagonist with anxiolytic and antidepressant activity in mice. *J Clin Invest* 2011; 121: 1846–1857.
31. Guzowski JF, Lyford GL, Stevenson GD, et al. Inhibition of activity-dependent arc protein expression in the rat hippocampus impairs the maintenance of long-term potentiation and the consolidation of long-term memory. *J Neurosci* 2000; 20: 3993–4001.
32. McIntyre CK, Miyashita T, Setlow B, et al. Memory-influencing intra-basolateral amygdala drug infusions modulate expression of Arc protein in the hippocampus. *Proc Natl Acad Sci U S A* 2005; 102: 10718–10723.
33. Ploski JE, Pierre VJ, Smucny J, et al. The activity-regulated cytoskeletal-associated protein (Arc/Arg3.1) is required for memory consolidation of pavlovian fear conditioning in the lateral amygdala. *J Neurosci* 2008; 28: 12383–12395.
34. Ahmadian G, Ju W, Liu L, et al. Tyrosine phosphorylation of GluR2 is required for insulin-stimulated AMPA receptor endocytosis and LTD. *EMBO J* 2004; 23: 1040–1050.
35. Velmeshev D, Magistri M and Faghihi MA. Expression of non-protein-coding antisense RNAs in genomic regions related to autism spectrum disorders. *Mol Autism* 2013; 4: 32.
36. Magistri M, Velmeshev D, Makhmutova M, et al. Transcriptomics profiling of Alzheimer's disease reveal neurovascular defects, altered amyloid-beta homeostasis, and deregulated expression of long noncoding RNAs. *J Alzheimers Dise* 2015; 48: 647–665.
37. Lange-Asschenfeldt C, Raval AP, Dave KR, et al. Epsilon protein kinase C mediated ischemic tolerance requires activation of the extracellular regulated kinase pathway in the organotypic hippocampal slice. *J Cereb Blood Flow Metab* 2004; 24: 636–645.
38. Tanaka E, Yamamoto S, Kudo Y, Mihara S and Higashi H. Mechanisms underlying the rapid depolarization produced by deprivation of oxygen and glucose in rat hippocampal CA1 neurons in vitro. *J Neurophysiol* 1997; 78: 891–902.
39. Raval AP, Dave KR, DeFazio RA, et al. epsilonPKC phosphorylates the mitochondrial K(+) (ATP) channel during induction of ischemic preconditioning in the rat hippocampus. *Brain Res* 2007; 1184: 345–353.
40. Morris-Blanco KC, Cohan CH, Neumann JT, et al. Protein kinase C epsilon regulates mitochondrial pools of Nampt and NAD following resveratrol and ischemic preconditioning in the rat cortex. *J Cereb Blood Flow Metab* 2014; 34: 1024–1032.
41. Morris-Blanco KC, Dave KR, Saul I, et al. Protein kinase C epsilon promotes cerebral ischemic tolerance via modulation of mitochondrial Sirt5. *Sci Rep* 2016; 6: 29790.
42. Korb E, Wilkinson CL, Delgado RN, et al. Arc in the nucleus regulates PML-dependent GluA1 transcription and homeostatic plasticity. *Nat Neurosci* 2013; 16: 874–883.
43. Maddox SA and Schafe GE. The activity-regulated cytoskeletal-associated protein (Arc/Arg3.1) is required for reconsolidation of a Pavlovian fear memory. *J Neurosci* 2011; 31: 7073–7082.
44. Liu Y, Zhou QX, Hou YY, et al. Actin polymerization-dependent increase in synaptic Arc/Arg3.1 expression in the amygdala is crucial for the expression of aversive memory associated with drug withdrawal. *J Neurosci* 2012; 32: 12005–12017.
45. Pietrobon D and Moskowitz MA. Chaos and commotion in the wake of cortical spreading depression and spreading depolarizations. *Nat Rev Neurosci* 2014; 15: 379–393.

46. Attwell D and Laughlin SB. An energy budget for signaling in the grey matter of the brain. *J Cereb Blood Flow Metab* 2001; 21: 1133–1145.
47. Dreier JP. The role of spreading depression, spreading depolarization and spreading ischemia in neurological disease. *Nat Med* 2011; 17: 439–447.
48. Allen NJ, Karadottir R and Attwell D. A preferential role for glycolysis in preventing the anoxic depolarization of rat hippocampal area CA1 pyramidal cells. *J Neurosci* 2005; 25: 848–859.
49. Henley JM, Barker EA and Glebov OO. Routes, destinations and delays: recent advances in AMPA receptor trafficking. *Trends Neurosci* 2011; 34: 258–268.
50. Lin DT, Makino Y, Sharma K, et al. Regulation of AMPA receptor extrasynaptic insertion by 4.1N, phosphorylation and palmitoylation. *Nat Neurosci* 2009; 12: 879–887.
51. Boehm J, Kang MG, Johnson RC, et al. Synaptic incorporation of AMPA receptors during LTP is controlled by a PKC phosphorylation site on GluR1. *Neuron* 2006; 51: 213–225.
52. Sheardown MJ, Suzdak PD and Nordholm L. AMPA, but not NMDA, receptor antagonism is neuroprotective in gerbil global ischaemia, even when delayed 24 h. *Eur J Pharmacol* 1993; 236: 347–353.
53. Kawasaki-Yatsugi S, Yatsugi S, Koshiya K, et al. Neuroprotective effect of YM90K, an AMPA-receptor antagonist, against delayed neuronal death induced by transient global cerebral ischemia in gerbils and rats. *Jpn J Pharmacol* 1997; 74: 253–260.
54. Walters MR, Kaste M, Lees KR, et al. The AMPA antagonist ZK 200775 in patients with acute ischaemic stroke: a double-blind, multicentre, placebo-controlled safety and tolerability study. *Cerebrovasc Dis* 2005; 20: 304–309.
55. Ghosh S, Reuveni I, Barkai E, et al. CaMKII activity is required for maintaining learning-induced enhancement of AMPAR-mediated synaptic excitation. *J Neurochem* 2016; 136: 1168–1176.
56. Goforth PB, Ren J, Schwartz BS, et al. Excitatory synaptic transmission and network activity are depressed following mechanical injury in cortical neurons. *J Neurophysiol* 2011; 105: 2350–2363.
57. Liu SJ and Zukin RS. Ca2+-permeable AMPA receptors in synaptic plasticity and neuronal death. *Trends Neurosci* 2007; 30: 126–134.
58. Mylroie H, Dumont O, Bauer A, et al. PKCepsilon-CREB-Nrf2 signalling induces HO-1 in the vascular endothelium and enhances resistance to inflammation and apoptosis. *Cardiovasc Res* 2015; 106: 509–519.
59. Bramham CR, Alme MN, Bittins M, et al. The Arc of synaptic memory. *Exp Brain Res* 2010; 200: 125–140.
60. Raval AP, Saul I, Dave KR, et al. Pretreatment with a single estradiol-17beta bolus activates cyclic-AMP response element binding protein and protects CA1 neurons against global cerebral ischemia. *Neuroscience* 2009; 160: 307–318.
61. Meller R, Minami M, Cameron JA, et al. CREB-mediated Bcl-2 protein expression after ischemic preconditioning. *J Cereb Blood Flow Metab* 2005; 25: 234–246.
62. Eliseev RA, Vanwinkle B, Rosier RN, et al. Diazoxide-mediated preconditioning against apoptosis involves activation of cAMP-response element-binding protein (CREB) and NFkappaB. *J Biolo Chem* 2004; 279: 46748–46754.
63. Lyford GL, Yamagata K, Kaufmann WE, et al. Arc, a growth factor and activity-regulated gene, encodes a novel cytoskeleton-associated protein that is enriched in neuronal dendrites. *Neuron* 1995; 14: 433–445.
64. Otsuka N, Tsuritani K, Sakurai T, et al. Transcriptional induction and translational inhibition of Arc and Cugbp2 in mice hippocampus after transient global ischemia under normothermic condition. *Brain Res* 2009; 1287: 136–145.